Journal of Sound and Vibration (1999) **227**(3), 555–586
Article No. jsvi.1999.2355, available online at http://www.idealibrary.com on IDEAL®

VISCOTHERMAL WAVE PROPAGATION INCLUDING ACOUSTO-ELASTIC INTERACTION, PART I: THEORY

W. M. BELTMAN

Department of Mechanical Engineering, University of Twente, P.O. Box 217, 7500 *AE Enschede, The Netherlands*

(*Received* 15 *December* 1998, *and in final form* 6 *May* 1999)

This research deals with pressure waves in a gas trapped in thin layers or narrow tubes. In these cases viscous and thermal effects can have a significant effect on the propagation of waves. This so-called viscothermal wave propagation is governed by a number of dimensionless parameters. The two most important parameters are the shear wave number and the reduced frequency. These parameters were used to put into perspective the models that were presented in the literature. The analysis shows that the complete parameter range is covered by three classes of models: the standard wave equation model, the low reduced frequency model and the full linearized Navier–Stokes model. For the majority of practical situations, the low reduced frequency model is sufficient and the most efficient to describe viscothermal wave propagation. The full linearized Navier–Stokes model should only be used under extreme conditions.

1. INTRODUCTION

The propagation of sound waves with viscothermal effects has been investigated in several scientific disciplines. The propagation of sound waves in tubes was investigated already by Kirchhoff and Rayleigh [1]. In *tribology*, the Reynolds equation is used to calculate the pressure distribution in fluid films trapped between moving surfaces. Reynolds' theory assumes that the inertial effects are negligible: it is based on a so-called creeping flow assumption. Increasing machine speeds and the use of gas bearings initiated research on the role of inertia [2–10]. In *fluid mechanics*, the propagation of sound waves in tubes and in particular the steady streaming phenomenon have been extensively discussed [11–14]. Two early papers on thin film theory in *acoustics* were presented by Maidanik [15] and Ungar and Carbonell [16]. A large number of investigations have been carried out since then. Consequently, a seemingly endless variety of models is available now to deal with viscothermal effects in acoustic wave propagation.

The variety of models is deceiving. The models that were presented in acoustics can be grouped into three basic categories. Key words in the characterization of these models are: pressure gradient across layer thickness or tube cross-section, and the incorporation of effects such as compressibility and thermal conductivity.

0022-460X/99/430555 + 32 $30.00/0

The most extensive type of model clearly must be based on a solution of the full set of basic equations. This means that, for instance, all the terms in the linearized Navier–Stokes equations are taken into account. The second type of model incorporates a pressure gradient. However, not all the terms in the basic equations are retained. In some models, for instance, thermal effects are neglected. The simplest model, the low reduced frequency model, assumes a constant pressure across the layer thickness or tube cross-section. The effects of inertia, viscosity, compressibility and thermal conductivity are accounted for. This leads to a very straightforward and useful model.

The main aim of this paper is to provide a framework for putting models for viscothermal wave propagation into perspective. It is not the intention of the author to present a list of all papers related to viscothermal wave propagation. Wave propagation is considered from a standard acoustical point of view. Non-linear effects are therefore neglected. For an extensive overview of non-linear effects and viscothermal wave propagation the reader is referred to the papers by Makarov and Ochmann [17–19] and Too and Lee [20]. Makarov and Ochmann present an overview of the literature, based on more than 300 references.

The present analysis is based on the use of dimensionless parameters. It is an extension of the work on the propagation of sound waves in cylindrical tubes, as presented by Tijdeman [21]. The three groups of models are all written in a dimensionless form. As a consequence, a number of dimensionless parameters appear in the equations. With the help of these parameters the range of validity for each group is indicated. Furthermore, for each type of model a short list of related literature is given. The list offers information about parameter ranges and applications. Based on this information, one can easily determine which model should be used for a given application. Finally, the problem of acoustic-elastic coupling, i.e., the mutual interaction between vibrating flexible surfaces and thin layers of gas or fluid, is addressed for each type of model.

2. BASIC EQUATIONS

2.1. DERIVATION OF EQUATIONS

The basic equations governing the propagation of sound waves are the linearized Navier–Stokes equations, the equation of continuity, the equation of state for an ideal gas and the energy equation. In the absence of mean flow the equations can be written as

$$\rho_0 \partial \bar{\mathbf{v}}/\partial t = -\bar{\nabla}\bar{p} + \left(\frac{4}{3}\mu + \eta\right)\bar{\nabla}(\bar{\nabla}\cdot\bar{\mathbf{v}}) - \mu\bar{\nabla}\times(\bar{\nabla}\times\bar{\mathbf{v}})$$

$$\rho_0(\bar{\nabla}\cdot\bar{\mathbf{v}}) + \partial\bar{\rho}/\partial t = 0, \quad \bar{p} = \bar{\rho} R_0 \bar{T},$$

$$\rho_0 C_p \partial \bar{T}/\partial t = \lambda \bar{\Delta}\bar{T} + \partial\bar{p}/\partial t, \tag{1}$$

where $\bar{\mathbf{v}}$, p, $\bar{\rho}$, $\bar{T}$, μ, η, R_0, ρ_0, λ, C_p and t denote respectively the velocity vector, pressure, density, temperature, viscosity, bulk viscosity,[†] gas constant, mean density, thermal conductivity, specific heat at constant pressure and time. The operators $\bar{\nabla}$ and $\bar{\Delta}$ are the gradient and the Laplace operator respectively. (A list of nomenclature is given in Appendix B).

The following assumptions are used: no internal heat generation; homogeneous medium: the dimensions and the wavelength have to be large compared to the mean free path—for air under standard atmospheric conditions this assumption breaks down for lengths smaller than 10^{-7} m or frequencies higher than 10^9 Hz; no mean flow; small, sinusoidal perturbations; laminar flow.[‡]

Dimensionless small harmonic perturbations are introduced according to

$$\bar{\mathbf{v}} = c_0 \mathbf{v} e^{i\omega t}, \quad \bar{p} = p_0[1 + p e^{i\omega t}], \quad \bar{T} = T_0[1 + T e^{i\omega t}], \quad \bar{\rho} = \rho_0[1 + \rho e^{i\omega t}], \tag{2}$$

where c_0, T_0, p_0, ω and i are the undisturbed speed of sound, the mean temperature, mean pressure, angular frequency and the imaginary unit. The gradient and the Laplace operators are non-dimensionalized with a length scale l. This length scale can, for example, represent the layer thickness or the tube radius. The other directions are scaled with the acoustic wavelength. An overview of length scales and operators for various geometries is given in Appendix A. At this stage one can write

$$\nabla = l\bar{\nabla}, \quad \Delta = l^2 \bar{\Delta}. \tag{3}$$

After further linearization the basic equation can be written in the following dimensionless form:[§]

$$i\mathbf{v} = -\frac{1}{k\gamma}\nabla p + \frac{1}{s^2}\left(\frac{4}{3} + \xi\right)\nabla(\nabla \cdot \mathbf{v}) - \frac{1}{s^2}\nabla \times (\nabla \times \mathbf{v}),$$

$$\nabla \cdot \mathbf{v} + i k\rho = 0, \quad p = \rho + T, \quad i T = \frac{1}{s^2\sigma^2}\Delta T + i\left[\frac{\gamma - 1}{\gamma}\right]p. \tag{4}$$

The following dimensionless parameters were introduced:[¶]

$$\text{shear wave number, } s = l\sqrt{\rho_0 \omega/\mu};$$

$$\text{reduced frequency, } k = \omega l/c_0;$$

$$\text{ratio of specific heats, } \gamma = \frac{C_p}{C_v};$$

$$\text{square root of the Prandtl number, } \sigma = \sqrt{\mu C_p/\lambda};$$

$$\text{viscosity ratio, } \xi = \eta/\mu\,. \tag{5}$$

[†]For monatomic gases $\eta = 0$, for air $\eta = 0{\cdot}6\mu$

[‡]For the transition to turbulence for oscillating pipe flows, see e.g. [14] and [72].

[§]$R_0 = C_p - C_v$

[¶]The shear wave number is an unsteady Reynolds number

Here, C_v is the specific heat at constant volume. The dimensionless equations indicate that the viscothermal wave propagation is governed by a number of dimensionless parameters. These parameters can be used to characterize different flow regimes. Furthermore, they enable solutions given in the literature to be put into perspective: assumptions or restrictions of models can be quantified in terms of these parameters.

The parameters γ and σ depend solely on the material properties of the gas. The most important parameters are the shear wave number and the reduced frequency. The shear wave number is a measure for the ratio between the inertial effects and the viscous effects in the gas: it is an unsteady Reynolds number. For large shear wave numbers the inertial effects dominate, whereas for low shear wave numbers the viscous effects are dominant. In physical terms the shear wave number represents the ratio between the length scale, e.g. the layer thickness or tube radius, and the boundary layer thickness. The reduced frequency represents the ratio between the length scale and the acoustic wavelength. For very low values of the reduced frequency, the acoustic wavelength is very large compared to the length scale l. The parameters presented in this section are essential for the choice of an appropriate model for a specific situation.

2.2. BOUNDARY CONDITIONS

In order to solve the set of equations boundary conditions must be imposed. The quantities of interest here are the (dimensionless amplitudes of the) velocity, temperature, pressure and density. Boundary conditions for the density are usually not imposed, and will therefore not be considered here.

2.2.1. *Velocity*

At a gas–wall interface, a continuity of velocity is assumed in most cases. Continuity of velocity usually implies that the tangential velocity is zero: a no-slip condition is imposed. The normal velocity is equal to the velocity of the wall. In this way, the acousto-elastic coupling between vibrating structures and viscothermal gases is established. For rarefied gases, investigations indicate that it is more appropriate to use a jump in velocity with corresponding momentum accommodation coefficients† [22, 23]. For gases under atmospheric conditions a simple continuity of velocity condition suffices.

2.2.2. *Temperature*

The most common boundary conditions are isothermal walls or adiabatic walls. For an isothermal wall the temperature perturbation is zero, whereas for an adiabatic wall the gradient of the temperature normal to the wall vanishes. When

†In this case one assumes a jump condition at the interface, e.g. a velocity slip or temperature jump. For the temperature the boundary equation then becomes: $T - T_w = -L\nabla T \cdot \mathbf{n}$, where T_w is the wall temperature, L is related to the thermal accommodation coefficients and $\mathbf{n}$ is the outward normal.

the product of the specific heat per unit volume and the thermal conductivity of the wall material substantially exceeds the corresponding product for the gas, the assumption of isothermal walls is usually accurate (see, e.g. reference [24]).

Again, for rarefied gases, it is more appropriate to use a jump condition [22, 23]. This condition allows for a jump in temperature across the gas–wall interface with a thermal accommodation coefficient. In the literature, some models were presented to model walls with finite heat conduction properties (see, Reference [25]).

A very interesting consequence of thermal effects is the phenomenon of thermally driven vibrations. As a boundary condition, one could for instance impose a varying temperature across the length of a tube. This temperature gradient drives pressure pulsations in the gas. This effect will not be addressed here: for detailed discussion the reader is referred to the literature [26–33].

2.2.3. *Pressure*

At the ends of a tube or layer boundary conditions can be imposed for the pressure, for instance a pressure release. In the present investigation end effects are neglected. For a more detailed discussion on this subject the reader is referred to the literature [34–39].

2.3. GEOMETRIES AND CO-ORDINATE SYSTEMS

The basic equations were given in terms of gradient and Laplace operators. In Appendix A an overview of length scales, dimensionless co-ordinates, gradient operators and Laplace operators is given for a number of geometries.

3. FULL LINEARIZED NAVIER–STOKES MODEL

3.1. DERIVATION OF EQUATIONS

The most extensive type of model is that obtained by solving the complete set of basic equations. The derivation in this section is based on the paper by Bruneau *et al.* [40]. Their formulation however was rewritten in terms of dimensionless quantities for the present study. In order to solve this problem, the velocity is written as the sum of a rotational velocity $\mathbf{v}_v$, due to viscous effects, and a solenoidal velocity $\mathbf{v}_l$

$$\mathbf{v} = \mathbf{v}_v + \mathbf{v}_l, \tag{6}$$

where these satisfy

$$\nabla \cdot \mathbf{v}_v = 0, \qquad \nabla \times \mathbf{v}_l = \mathbf{0}. \tag{7}$$

The following relationship was used in this derivation:

$$\nabla \times (\nabla \times \mathbf{v}_v) \equiv \nabla (\nabla \cdot \mathbf{v}_v) - (\nabla \cdot \nabla)\mathbf{v}_v = -\Delta \mathbf{v}_v. \tag{8}$$

Inserting these expressions into the basic equations and taking the rotation and divergence gives the following set of dimensionless equations:

$$\mathrm{i}\mathbf{v}_l - \frac{1}{s^2}\left(\frac{4}{3} + \boldsymbol{\xi}\right)\Delta\,\mathbf{v}_l = -\frac{1}{k\gamma}\,\nabla p,$$

$$\nabla\cdot\mathbf{v}_l + \mathrm{i}k\rho = 0, \quad \mathrm{i}\,\mathbf{v}_v - \frac{1}{s^2}\,\Delta\mathbf{v}_v = \mathbf{0}, \quad p = \rho + T, \quad \mathrm{i}\,T = \frac{1}{s^2\sigma^2}\,\Delta T + \mathrm{i}\left[\frac{\gamma-1}{\gamma}\right]p. \tag{9}$$

After some algebraic manipulations the following equation can be derived in terms of the temperature perturbation:

$$\frac{\mathrm{i}}{s^2\sigma^2}\left[1 + \frac{\mathrm{i}\gamma k^2}{s^2}\left(\frac{4}{3} + \boldsymbol{\xi}\right)\right]\Delta\Delta T + \left[1 + \frac{\mathrm{i}k^2}{s^2}\left(\frac{4}{3} + \boldsymbol{\xi}\right) + \frac{\gamma}{\sigma^2}\right]\Delta T + k^2\,T = 0. \tag{10}$$

It can easily be verified that both $\mathbf{v}_l$ and p also satisfy this equation. Note that if $\xi = 0$ in this equation, i.e., the bulk viscosity is neglected, a dimensionless equation is obtained that was already derived by Kirchhoff and Rayleigh [1].

3.2. SOLUTION STRATEGY

The equation for the temperature perturbation can be written in a factorized form,

$$[\Delta + k_a^2]\,[\Delta + k_h^2]\,T = 0, \tag{11}$$

where k_a and k_h are the acoustic and entropic wave numbers respectively,

$$k_a^2 = \frac{2k^2}{C_1 + \sqrt{C_1^2 - 4C_2}}, \qquad k_h^2 = \frac{2k^2}{C_1 - \sqrt{C_1^2 - 4C_2}}, \tag{12}$$

in which:

$$C_1 = \left[1 + \frac{\mathrm{i}k^2}{s^2}\left[\left(\frac{4}{3} + \xi\right) + \frac{\gamma}{\sigma^2}\right]\right], \qquad C_2 = \frac{\mathrm{i}k^2}{s^2\sigma^2}\left[1 + \frac{\mathrm{i}\gamma k^2}{s^2}\left(\frac{4}{3} + \xi\right)\right]. \tag{13}$$

The solution for the temperature perturbation can be written as

$$T = A_a T_a + A_h T_h, \tag{14}$$

where T_a and T_h are referred to as the acoustic and the entropic temperatures. The constants A_a and A_h remain to be determined from the boundary conditions. The quantities T_a and T_h are the solutions of

$$[\Delta + k_a^2]\,T_a = 0, \qquad [\Delta + k_h^2]\,T_h = 0. \tag{15}$$

Once the solution for the temperature is known, the values for the velocity $\mathbf{v}_l$ and the pressure p can be expressed in terms of A_a, A_h, T_a and T_a. One obtains

$$p = \left[\frac{\gamma}{\gamma-1}\right]\left[A_a\left[1 - \frac{\mathrm{i}k_a^2}{s^2}\frac{1}{\sigma^2}\right]T_a + A_h\left[1 - \frac{\mathrm{i}k_h^2}{s^2}\frac{1}{\sigma^2}\right]T_h\right],$$

$$\mathbf{v}_l = \mathbf{v}_{la} + \mathbf{v}_{lh} = \alpha_a A_a \nabla T_a + \alpha_h A_h \nabla T_h,$$

$$\alpha_a = \frac{\mathrm{i}}{k\gamma}\left[\frac{\gamma}{\gamma-1}\right]\left[\frac{1-\dfrac{\mathrm{i}k_a^2}{s^2}\dfrac{1}{\sigma^2}}{1-\dfrac{\mathrm{i}k_a^2}{s^2}\left(\dfrac{4}{3}+\xi\right)}\right], \qquad \alpha_h = \frac{\mathrm{i}}{k\gamma}\left[\frac{\gamma}{\gamma-1}\right]\left[\frac{1-\dfrac{\mathrm{i}k_k^2}{s^2}\dfrac{1}{\sigma^2}}{1-\dfrac{\mathrm{i}k_k^2}{s^2}\left(\dfrac{3}{4}+\xi\right)}\right]. \tag{16}$$

The rotational velocity $\mathbf{v}_v$ has to be solved for from a vector wave equation with wave number k_v:

$$[\Delta + k_v^2]\mathbf{v}_v = \mathbf{0}, \qquad k_v^2 = -\mathrm{i}s^2. \tag{17}$$

The rotational velocity is related to the effects of viscosity, since the wave number is a function of the shear wave number.

In order to solve the full model, solutions must be found to two *scalar wave equations* for the temperature perturbation and a *vector wave equation* for the rotational velocity. With the appropriate boundary conditions the complete solution can then be obtained. An analytical solution for this type of model can be found only for simple geometries and boundary conditions. For more complex geometries one has to resort to numerical techniques.

3.3. ACOUSTIC AND ENTROPIC WAVE NUMBERS

The expressions for k_a and k_h are rather complex. In the literature they are often approximated; see e.g., reference [40]. With the help of the dimensionless parameters this approximation can be quantified. A Taylor expansion of the denominator of the wave numbers in terms of k/s gives

$$k_a^2 = \frac{k^2}{\left[1+\mathrm{i}\left(\dfrac{k}{s}\right)^2\left[\left(\dfrac{4}{3}+\xi\right)+\dfrac{\gamma-1}{\sigma^2}\right]-\left(\dfrac{k}{s}\right)^4\left(\dfrac{\gamma-1}{\sigma^2}\right)\left[\dfrac{1}{\sigma^2}-\left(\dfrac{4}{3}+\xi\right)\right]\right]},$$

$$k_h^2 = \frac{-\mathrm{i}s^2\sigma^2}{\left[1-\mathrm{i}(\gamma-1)\left(\dfrac{k}{s}\right)^2\left[\dfrac{1}{\sigma^2}-\left(\dfrac{4}{3}+\xi\right)\right]\right]}. \tag{18}$$

These expressions are valid for $k/s \ll 1$: the acoustic wavelength is very large compared to the boundary layers thicknesses. This assumption seems very reasonable. However, it has important implications that actually eliminate the need for a full model, as will also be illustrated in section 5.5. If one sets $k/s = 0$ the expressions reduce to

$$k_a^2 = k^2, \qquad k_h^2 = -\mathrm{i}s^2\sigma^2. \tag{19}$$

This result shows that the wave number k_a is related to acoustic effects. The wave number k_h is related to entropy effects, since the product $s\sigma$ does not contain the

viscosity μ. However, this separation is possible only for $k/s \ll 1$. When the acoustic wavelength is of the same order of magnitude as the boundary layer thickness, the complete expressions for the wave numbers k_a and k_h must be used. In this situation a separation is not possible.

Note that for $s \gg 1$ the wave numbers k_h and k_v become very large. The solutions for T_h and $\mathbf{v}_v$ approach zero. The value of k_a is not affected, since it is not a function of the shear wave number. As a consequence, the full linearized Navier–Stokes model reduces to the standard wave equation.

3.4. ACOUSTO-ELASTIC COUPLING

The motion of the gas can be coupled to the motion of a flexible structure, usually by demanding a continuity of velocity across the interface. In general, this leads to a very complicated set of equations. The full linearized Navier–Stokes model was used in a number of applications, such as spherical resonators or miniaturized transducers, to calculate the acousto-elastic behaviour of systems.

Spherical resonators are used to determine the acoustical properties of gases with a high degree of accuracy. Mehl investigated the effect of shell motion, hereby neglecting viscothermal effects in the gas [41]. Moldover *et al.* [24] used a full linearized Navier–Stokes model for the description of the acoustic field inside the resonator. A boundary impedance condition was imposed for the radial velocity in order to account for the effect of shell motion. The models developed by Mehl were used to calculate this shell impedance.

In some types of *miniaturized transducers* a vibrating membrane is backed by a rigid electrode, thus entraping a thin layer of gas. Plantier and Bruneau [42], Bruneau, *et al.* [43], and Hamery *et al.* [44] developed analytical models to describe the interaction between (circular) membranes and thin gas layers. Because of the complexity of the problem, their calculations are restricted to geometries with rotatory symmetry. In order to overcome this problem, recently Karra *et al.* [45, 46] presented a boundary element formulation for the propagation of sound waves in viscothermal gases. Although their paper concerns only an uncoupled test case and did not include viscous effects, the algorithm is able to deal with fully coupled problems [47]. Their method therefore now offers the possibility to model more complex geometries.

In Part II of the present paper the spherical resonator and the miniaturized transducers are discussed in more detail.

3.5. LITERATURE

In Table 1 a list of related literature is presented. The list contains information concerning applications and acousto-elastic coupling. For layer geometries the parameter ranges in the calculations and experiments are given. These values will also be used in section 5.5. For an overview of parameter values for tubes the reader is referred to the paper by Tijdeman [21].

TABLE 1

Literature full linearized Navier–Stokes models (•): *calculations*

Authors	Ref	Year	Application	Coupling	Remarks
Moldover *et al.*	[24]	1986	Spherical resonator	Full	Analytical model
Bruneau *et al.*	[69]	1990	Spherical resonator Cylindrical tubes	No	Analytical model
Plantier and Bruneau	[42]	1990	Circular membrane	Full	Analytical model $2{\cdot}3\times10^{-9}\leqslant k\leqslant 2{\cdot}3\times10^{-3}$ (•) $2{\cdot}9\times10^{-6}\leqslant k/s\leqslant 2{\cdot}9\times10^{-3}$ (•)
Bruneau	[70]	1994	Membrane	No	Analytical model
Hamery *et al.*	[44]	1994	Circular membrane	Full	Analytical model $4{\cdot}6\times10^{-5}\leqslant k\leqslant 4{\cdot}6\times10^{-2}$ (•) $9{\cdot}0\times10^{-4}\leqslant k/s\leqslant 2{\cdot}8\times10^{-2}$ (•)
Bruneau *et al.*	[40]	1989	Spherical resonator cylindrical tube plane wall	No	Analytical models
Bruneau *et al.*	[71]	1987	Tubes	No	Analytical model
Karra *et al.*	[45]	1996	Circular membrane	No	Boundary element model $7{\cdot}9\times10^{-3}\leqslant k\leqslant 1{\cdot}4\times10^{-2}$ (•) $8{\cdot}5\times10^{-3}\leqslant k/s\leqslant 1{\cdot}1\times10^{-2}$ (•)
Karra and Tahar	[46]	1997	Circular membrane	No	Boundary element model Case I ($h_0=0{\cdot}5$ mm): $1{\cdot}0\leqslant k\leqslant 1{\cdot}4$ (•) $9{\cdot}9\times10^{-3}\pm k/s\leqslant 1{\cdot}1\times10^{-2}$ (•) Case II ($h_0=1$ μm): $7{\cdot}9\times10^{-3}\leqslant k\leqslant 1{\cdot}4\times10^{-2}$ (•) $2{\cdot}7\times10^{-2}\leqslant k/s\leqslant 3{\cdot}6\times10^{-2}$ (•)
Scarton and Rouleau	[72]	1973	Tubes	No	
Tijdeman	[21]	1975	Tubes	No	
Liang and Scarton	[73]	1994	Tubes	No	

4. SIMPLIFIED NAVIER–STOKES MODELS

In this class of models, the effects of compressibility or thermal conductivity are neglected compared with the full model described in section 2.3. In this section, two models will be discussed in more detail. The two models were rewritten in a dimensionless form for this purpose. Other models are also available, but all simplified Navier–Stokes models are inconsistent. An overview is presented in section 4.4.

4.1. TROCHIDIS MODEL

Trochidis [48, 49] introduced the following assumption in addition to the basic assumptions described in section 2.1: the gas is incompressible: $\nabla \cdot \mathbf{v} = 0$. The dimensionless basic equations (4) now reduce to†

$$\mathrm{i}\mathbf{v} = -\frac{1}{k\gamma}\nabla p - \frac{1}{s^2}\nabla \times (\nabla \times \mathbf{v}), \quad \nabla \cdot \mathbf{v} = 0. \tag{20}$$

Combining these equations gives

$$\Delta p = 0, \quad [\Delta - \mathrm{i}s^2]\,\mathbf{v} = \frac{s^2}{k\gamma}\nabla p. \tag{21}$$

The equation for the pressure is perhaps strange at first sight. Is does not incorporate any viscothermal terms: it is a regular wave equation for incompressible gas behaviour. It seems that the pressure can be completely determined from this equation. However, the boundary conditions must be satisfied. At a gas–wall interface the velocity must be continuous. Usually, this means that the tangential velocity is zero and the normal velocity equals the velocity of the wall. With equation (21) the boundary condition for the velocity can be expressed in terms of pressure gradients. In this way, viscous effects are introduced into the model.

Clearly, the full linearized Navier–Stokes model reduces to the Trochidis model for incompressible behaviour. The role of the compressibility depends, among other things, on for example the frequency and the global dimensions. As an example, consider the squeeze film damping between two plates, as described by Trochidis. The effects of compressibility become important when the acoustic wavelength is of the same order of magnitude as the plate dimensions. This means that the incompressible model of Trochidis can only be used for frequencies for which the acoustic wavelength is very large compared to the plate dimensions. In a squeeze film problem, the layer thickness is very small compared to the plate dimensions. In other words, the acoustic wavelength is also very large compared to the layer thickness. The pressure will thus not vary much across the layer thickness. The Trochidis model however incorporates a pressure gradient across the layer thickness. This is a weakness of the model: the assumption of incompressible

†The 2D formulation from Trochidis was extended to 3D for the present analysis.

behaviour on the one hand and the incorporation of a pressure gradient across the layer on the other hand are rather inconsistent for a squeeze film problem.

4.2. MÖSER MODEL

Möser [50] extended the Trochidis model in order to account for the compressibility of the gas. However, only the compressibility term in the equation of continuity is considered: the compressibility terms in the linearized Navier–Stokes equations are neglected. Furthermore, the process is assumed to be adiabatic. Möser in fact introduced the following assumptions in addition to the basic assumptions described in section 2.1: incompressible linearized Navier–Stokes equations; adiabatic process. The basic equations (4) now reduce to†

$$\mathrm{i}\mathbf{v} = -\frac{1}{k\gamma}\nabla\mathbf{p} - \frac{1}{s^2}\nabla\times(\nabla\times\mathbf{v}), \quad \nabla\cdot\mathbf{v} + \mathrm{i}k\rho = 0, \quad p = \gamma\rho. \tag{22}$$

Combining these equations gives

$$\Delta p + \left[\frac{k^2}{1+\mathrm{i}\left(\frac{k}{s}\right)^2}\right] p = 0, \quad \Delta(\nabla\times\mathbf{v}) - \mathrm{i}s^2(\nabla\times\mathbf{v}) = \mathbf{0}. \tag{23}$$

In a further analysis, Möser assumed that the acoustic wavelength is very large compared to the boundary layer thickness: $k/s \ll 1$. The wave number in equation (23) then reduces to k^2 and thus the equation reduces to the standard wave equation. In this model, the viscous effects are also incorporated through the boundary conditions, if the wave number is approximated by k^2.

This model is not very consistent, since the compressibility terms are not fully accounted for. Furthermore, the thermal effects can play an important role. There are indeed several examples where thermal effects do have a significant influence. For a more sophisticated model that incorporate pressure gradients, the thermal effects should be accounted for as well.

4.3. ACOUSTO-ELASTIC COUPLING

In acoustics, the simplified Navier–Stokes models were mainly used to calculate the squeeze film damping between flexible plates. In the analysis of Trochidis only one-way coupling is considered: the uncoupled deflections of the plates were imposed as boundary conditions for the gas. However, recent experiments and calculations [51, 52] indicate that thin gas layers can have a significant effect on the coupled vibrational behaviour of a plate–gas layer system. The eigenfrequencies of the plate are substantially affected by the presence of the layer, whereas the viscothermal effects induce considerable damping. The full coupling was accounted

†The 2D formulation from Möser was extended to 3D for the present analysis.

for in the analysis of Möser. It has to be noted that the models as presented by Trochidis and Möser concern two-dimensional problems.

The interaction between viscous fluids and flexible structures was also investigated from a more mathematical point of view. Schulkes [53] presented a finite element method to describe the interaction between a viscous fluid and a flexible structure. He assumed the fluid to be incompressible. For more literature related to this topic the reader is referred to the papers by Schulkes [53, 54].

4.4. LITERATURE

In Table 2 a list of papers concerning simplified Navier–Stokes models is presented. Experiments were carried out by several authors. The parameter ranges for the layer geometries are also given in the table.

5. LOW REDUCED FREQUENCY MODEL

5.1. DERIVATION OF EQUATIONS

In the low reduced frequency models some simplifications are introduced that lead to a relatively simple but very useful model for tubes and layers. In this theory, the propagation directions of the waves and the other directions are separated. The following assumptions are introduced in addition to the basic assumptions described in section 2.1: the acoustic wavelength is large compared to the length scale l: $k \ll 1$; the acoustic wavelength is large compared to the boundary layer thickness: $k/s \ll 1$. If one introduces these assumptions into the basic equations (4), presented in section 2.1, one is left with[†]

$$\mathrm{i}\mathbf{v}^{pd} = -\frac{1}{k\gamma}\nabla^{pd}p + \frac{1}{s^2}\Delta^{cd}\mathbf{v}^{pd}, \quad 0 = -\frac{1}{k\gamma}\nabla^{cd}p, \quad \nabla\cdot\mathbf{v} + \mathrm{i}k\rho = 0,$$

$$p = \rho + T, \quad \mathrm{i}T = \frac{1}{s^2\sigma^2}\Delta^{cd}T + \mathrm{i}\left[\frac{\gamma-1}{\gamma}\right]p, \tag{24}$$

where ∇^{pd}, Δ^{pd} and $\mathbf{v}^{pd}$ represent the gradient operator, the Laplace operator and the velocity vector containing components for the propagation directions only. The operators ∇^{cd}, Δ^{cd} and $\mathbf{v}^{cd}$ contain terms for the other directions, i.e., the cross-sectional or thickness directions. Expressions for these operators for various geometries are given in Appendix A.[‡] The cross-sectional co-ordinates are denoted by $\mathbf{x}^{cd}$ and the propagation co-ordinates are denoted by $\mathbf{x}^{pd}$.

[†]If not the acoustic wave length is the appropriate length scale for the *pd*-directions but a characteristic dimension L, one can show that the conditions $k \ll 1$, $k/s \ll 1$ and $l/L \ll 1$ have to hold. For thin layers or narrow tubes this geometric condition is implicitly satisfied. Calculations indicate that the low reduced frequency model can be used for $l/L < 0{\cdot}2$.

[‡]Note that a low reduced frequency model does not make sense for a spherical geometry.

TABLE 2

Literature simplified Navier–Stokes models (○): *experiments*, (•): *calculations*

Authors	Ref	Year	Application	Coupling	Remarks
Trochidis	[48]	1982	Squeeze film	One-way	Incompressible Case I (air): $4{\cdot}6\times10^{-4}\leqslant k\leqslant 8{\cdot}8\times10^{-2}$ (○) (•) $2{\cdot}8\times10^{-4}\leqslant k/s\leqslant 2{\cdot}3\times10^{-3}$ (○) (•) Case II (water): $5{\cdot}3\times10^{-4}\leqslant k\leqslant 4{\cdot}0\times10^{-2}$ (○) (•) $1{\cdot}7\times10^{-5}\leqslant k/s\leqslant 1{\cdot}3\times10^{-4}$ (○) (•)
Möser	[50]	1980	Squeeze film	Full	Incompressible Navier–Stokes $2{\cdot}3\times10^{-5}\leqslant k\leqslant 2{\cdot}9\times10^{-1}$ (•) $9{\cdot}0\times10^{-5}\leqslant k/s\leqslant 5{\cdot}1\times10^{-3}$ (•)
Schulkes	[53]	1990	General	Full	Incompressible
Chow and Pinnington	[67]	1987	Squeeze film (gas)	One way	Bulk viscosity terms neglected Thermal effects neglected Case I (atmospheric air): $2{\cdot}3\times10^{-4}\leqslant k\leqslant 7{\cdot}3\times10^{-2}$ (○) (•) $2{\cdot}9\times10^{-4}\leqslant k/s\leqslant 2{\cdot}9\times10^{-3}$ (○) (•) Case II (air, decompression chamber): $3{\cdot}5\times10^{-4}\leqslant k\leqslant 3{\cdot}5\times10^{-2}$ (○) (•) $2{\cdot}9\times10^{-4}\leqslant k/s\leqslant 4{\cdot}9\times10^{-3}$ (○) (•)
Chow and Pinnington	[68]	1989	Squeeze film (fluid)	One-way	Bulk viscosity terms neglected Thermal effects neglected $5{\cdot}2\times10^{-5}\leqslant k\leqslant 1{\cdot}3\times10^{-1}$ (○) (•) $2{\cdot}4\times10^{-5}\leqslant k/s\leqslant 2{\cdot}4\times10^{-4}$ (○) (•)

5.2. SOLUTION STRATEGY

The second of equations (24) indicates that the pressure is a function of the propagation co-ordinates only: the pressure is constant on a cross section or across the layer thickness. Hence, the low reduced frequency models are sometimes referred to as constant pressure models. By using the fact that the pressure does not vary with the *cd* co-ordinates, the temperature perturbation can be solved from a Poisson type of equation. The general solution for adiabatic or isothermal walls can formally be obtained by the Green function.† At this stage one can write

$$T(s\sigma, \mathbf{x}^{pd}, \mathbf{x}^{cd}) = -\left[\frac{\gamma - 1}{\gamma}\right] p(\mathbf{x}^{pd}) C(s\sigma, \mathbf{x}^{cd}). \tag{25}$$

For simple geometries, solution of the function C is very straightforward.‡ For more complex geometries numerical techniques can be used. In the literature, several approximation techniques have been developed to describe the propagation of sound waves in tubes with arbitrary cross-sections; see e.g., references [55–57]. Once the solution for the temperature is obtained, the solutions for the velocity and the density can be expressed in a similar way:

$$\mathbf{v}^{pd}(s, \mathbf{x}^{pd}, \mathbf{x}^{cd}) = -\frac{\mathrm{i}}{k\gamma} A(s, \mathbf{x}^{cd}) \nabla^{pd} p(\mathbf{x}^{pd}),$$

$$\rho(s\sigma, \mathbf{x}^{pd}, \mathbf{x}^{cd}) = p(\mathbf{x}^{pd}) \left[1 + \left[\frac{\gamma - 1}{\gamma}\right] C(s\sigma, \mathbf{x}^{cd})\right]. \tag{26}$$

Note that, due to the fact that A and C are functions of the *cd*-co-ordinates, the velocity, temperature and density are not constant in these directions. The functions A and C determine the shape of the velocity, temperature and density profiles. For isothermal walls the functions A and C are directly related, whereas for adiabatic walls the function C reduces to a very simple form. One has

$$\text{isothermal walls,} \quad C(s\sigma, \mathbf{x}^{cd}) = A(s\sigma, \mathbf{x}^{cd});$$

$$\text{adiabatic walls,} \quad C(s\sigma, \mathbf{x}^{cd}) = -1. \tag{27}$$

The expressions for ρ, T and $\mathbf{v}^{pd}$ are now inserted into the equation of continuity. After integration with respect to the *cd*-co-ordinates and some rearranging one obtains

$$\Delta^{pd} p(\mathbf{x}^{pd}) - k^2 \Gamma^2 p(\mathbf{x}^{pd}) = -\mathrm{i}kn(s\sigma) \Gamma^2 \mathfrak{R} \tag{28}$$

where

$$\Gamma = \sqrt{\frac{\gamma}{n(s\sigma) B(s)}}, \quad n(s\sigma) = \left[1 + \left[\frac{\gamma - 1}{\gamma}\right] D(s\sigma)\right]^{-1}$$

†It is also possible to include a finite thermal conductivity of the wall, see e.g. section 2.2.2. and reference [40]. The low reduced frequency model has to be coupled to a model that describes the thermal behaviour of the wall.

‡The function C is a function only of the *cd*-co-ordinates for constant cross-sections. For varying cross sections, the value of C depends also on the *pd*-co-ordinates.

$$B(s) = \frac{1}{A^{cd}} \int_{A^{cd}} A(s, \mathbf{x}^{cd}) \mathrm{d}A^{cd}, \quad D(s\sigma) = \frac{1}{A^{cd}} \int_{A^{cd}} C(s\sigma, \mathbf{x}^{cd}) \mathrm{d}A^{cd},$$

$$\mathfrak{R} = \frac{1}{A^{cd}} \int_{\partial A^{cd}} \mathbf{v} \cdot \mathbf{e}_n \mathrm{d}\partial A^{cd}. \tag{29}$$

where A^{cd} is the cross-sectional area, ∂A^{cd} is the corresponding boundary and $\mathbf{e}_n$ is the outward normal on ∂A^{cd}. For simple boundary conditions, the function D can be obtained from

$$\text{isothermal walls,} \quad D(s\sigma) = B(s\sigma); \quad \text{adiabatic walls,} \quad D(s\sigma) = -1. \tag{30}$$

The function Γ is the *propagation constant*. The propagation of sound waves is affected by thermal effects, accounted for in the function $n(s\sigma)$, and viscous effects, accounted for in the function $B(s)$. On the right hand side of equation (28) a source term is present due to the squeeze motion of the walls. In Tables A.1–A.4 in Appendix A the expressions are listed for various geometries and isothermal wall conditions for the functions A and B. The tables also contain the asymptotic values of the functions for low and high values of the corresponding argument. It can easily be shown that for low values of the shear wave number† the low reduced frequency model reduces to a linearized form of the Reynolds equation. For high shear wave numbers the low reduced frequency model reduces to a modified form of the wave equation. The modification is due to the fact that the low reduced frequency model is associated with a constant pressure in the cd-directions.

5.3. PHYSICAL INTERPRETATION

5.3.1 *Velocity profile*

The shape of the velocity profile is completely determined by the function A. This function is thus well suited to illustrate the transition from inertially dominated flow to viscously dominated flow. As an example, consider the layer geometry. In Figure 1 the magnitude of the function A is given as a function of the layer thickness for shear wave numbers 1, 5, 10 and 100. The magnitude of the function A is directly related to the magnitude of the in-plane velocities for a layer geometry. Note that the expression for the velocity is complex: there are phase differences between the points. Consequently not all points pass their equilibrium position at the same time.

For low shear wave numbers the viscous forces dominate and a parabolic velocity profile is obtained, see also Tables A.3 and A.4. For high shear wave numbers the inertial forces dominate and a flat velocity profile is obtained.

5.3.2. *Temperature profile*

For isothermal walls the shape of the temperature profile is identical to the shape of the velocity profile. However, the temperature is not a function of the shear wave

†Considering σ as a constant.

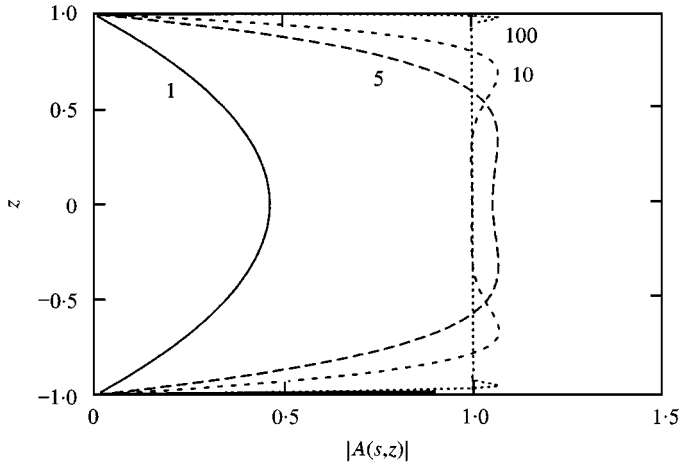

Figure 1. Shape of velocity profile (magnitude).

number s but of the product $s\sigma$: its value does not depend on the viscosity μ. For high values of $s\sigma$, adiabatic conditions are obtained, whereas for low values of $s\sigma$, isothermal conditions are obtained.

5.3.3. *Polytropic constant*

According to equation (26) the density and the pressure are related. If this expression is integrated with respect to the *cd*-co-ordinates one obtains

$$\rho = p\left[1 + \left[\frac{\gamma - 1}{\gamma}\right] D(s\sigma)\right]. \tag{31}$$

The same result would have been obtained if, instead of using the energy equation and the equation of state, a polytropic law had been used, namely,

$$\bar{p}/\bar{\rho}^{n(s\sigma)} = \text{constant}, \tag{32}$$

where $n(s\sigma)$ is the polytropic constant that relates density and pressure, see equation (29). Note however that this only holds in integrated sense: relation (31) was obtained by integration with respect to the *cd*-co-ordinates. As an example, the magnitude and the phase angle for the layer geometry are given as a function of $s\sigma$ in Figure 2. For low values $n(s\sigma)$ reduces to 1, i.e., isothermal conditions. For high values of $s\sigma$ it takes the value of γ corresponding to adiabatic conditions.

5.4. ACOUSTO-ELASTIC COUPLING

The low reduced frequency model results in a relatively simple equation for the pressure. Because of the simplicity of the gas model, it is relatively easy to incorporate the full acousto-elastic coupling. Several investigations are available which deal with fully coupled calculations, most of them for the squeeze film problem.

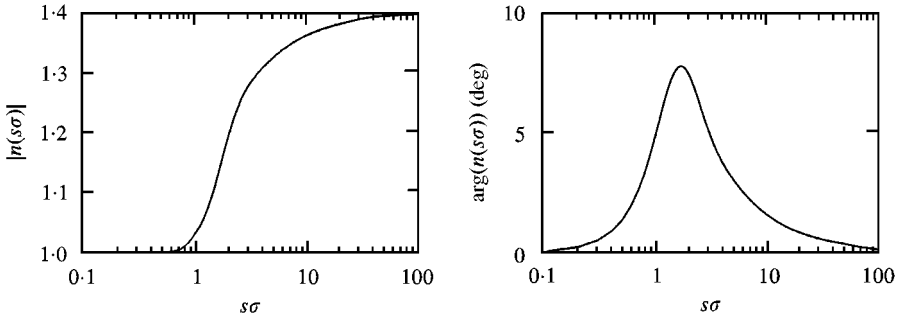

Figure 2. Magnitude and phase angle of polytropic constant for air ($\gamma = 1{\cdot}4$).

Fox and Whitton [58] and Önsay [59, 60] presented models to describe the interaction between a vibrating strip and a gas layer. The model of Önsay was based on a transfer matrix approach: an efficient model for the strip problem. Fox and Whitton, and Önsay, carried out experiments, showing substantial frequency shifts and significant damping. Lotton *et al.* [61] and Bruneau *et al.* [62] and Bruneau *et al.* [63] studied the behaviour of circular and rectangular membranes, backed by a thin gas layer.

Recently, Beltman *et al.* [51, 52, 64–66] presented a finite element model for fully coupled calculations for the squeeze film problem. A new viscothermal acoustic finite element was developed, based on the low reduced frequency model. This element can be coupled to structural elements, enabling fully coupled calculations to be made for complex geometries. Furthermore, the layer thickness can be chosen for each element. This enables calculations for problems with varying layer thickness. The finite element model was validated with experiments on an airtight box with a flexible overplate. In this case there was a strong interaction between the vibrating, flexible plate and the closed air layer. Eigenfrequency and damping of the plate were measured as a function of the thickness of the air layer. Substantial frequency shifts and large damping values were observed.

5.5. LITERATURE

In Table 3, the recent literature on the low reduced frequency models is summarized. For layer geometries the ranges of dimensionless parameters are also given.

6. DIMENSIONLESS PARAMETERS

6.1. VALIDITY OF MODELS

In sections 2.3, 3.5 and 4.4, three types of models were discussed for the modelling of viscothermal wave propagation. The most simple type of model, the low reduced frequency model, was shown to be valid for $k \ll 1$ and $k/s \ll 1$. As pointed out in section 3.5, the validity of the simplified Navier–Stokes models is difficult to

TABLE 3

Literature low reduced frequency model. (○): *experiments*, (•): *calculations*

Authors	Ref	Year	Application	Coupling	Remarks
Fox and Whitton	[58]	1980	Squeeze film (strip)	Full	Analytical model Case I (atmospheric air): $1{\cdot}8\times10^{-3}\leqslant k\leqslant 1{\cdot}8\times10^{-1}$ (○) (•) $k/s\cong 4{\cdot}0\cdot10^{-4}$ (○) (•) Case II (air, decompression chamber): $1{\cdot}2\times10^{-4}\leqslant k\leqslant 4{\cdot}6\cdot10^{-4}$ (○) (•) $9{\cdot}2\times10^{-5}\leqslant k/s\leqslant 4{\cdot}1\cdot10^{-3}$ (○) (•) Case III (CO_2 decompression chamber): $2{\cdot}3\times10^{-4}\leqslant k\leqslant 3{\cdot}1\cdot10^{-4}$ (○) (•) $1{\cdot}0\times10^{-4}\leqslant k/s\leqslant 3{\cdot}8\cdot10^{-3}$ (○) (•)
Onsay	[59]	1993	Squeeze film (strip)	Full	Transfer matrix approach $9{\cdot}2\times10^{-6}\leqslant k\leqslant 4{\cdot}6\cdot10^{-3}$ (○) (•) $9{\cdot}0\times10^{-5}\leqslant k/s\leqslant 9{\cdot}0\cdot10^{-4}$ (○) (•)
Onsay	[60]	1994	Squeeze film (strip)	Full	Step in layer geometry $9{\cdot}2\cdot10^{-5}\leqslant k\leqslant 4{\cdot}6\cdot10^{-3}$ (○) (•) $9{\cdot}0\cdot10^{-5}\leqslant k/s\leqslant 9{\cdot}0\cdot10^{-4}$ (○) (•)
Lotton *et al.*	[70]	1994	Circular membrane	Full	Equivalent network model
Bruneau *et al.*	[62]	1994	Circular membrane	Full	Equivalent network model
Bruneau *et al.*	[63]	1994	Rectangular membrane	Full	$6{\cdot}9\cdot10^{-7}\leqslant k\leqslant 6{\cdot}9\cdot10^{-2}$ (•) $9{\cdot}1\cdot10^{-5}\leqslant k/s\leqslant 2{\cdot}9\cdot10^{-2}$ (•)
Tijdeman	[21]	1975	Tubes	No	Parameter overview
Beltman *et al.*	[52]	1997	Squeeze film (plate)	Full	Finite element model $4{\cdot}6\times10^{-4}\leqslant k\leqslant 1{\cdot}4\cdot10^{-1}$ (○) (•) $2{\cdot}0\times10^{-4}\leqslant k/s\leqslant 4{\cdot}9\cdot10^{-4}$ (○) (•)
Beltman *et al.*	[64]	1997	Solar panels	No	Analytical model $1{\cdot}8\cdot10^{-5}\leqslant k\leqslant 6{\cdot}0\cdot10^{-2}$ (○) (•) $2{\cdot}9\cdot10^{-5}\leqslant k/s\leqslant 9{\cdot}0\cdot10^{-5}$ (○) (•)

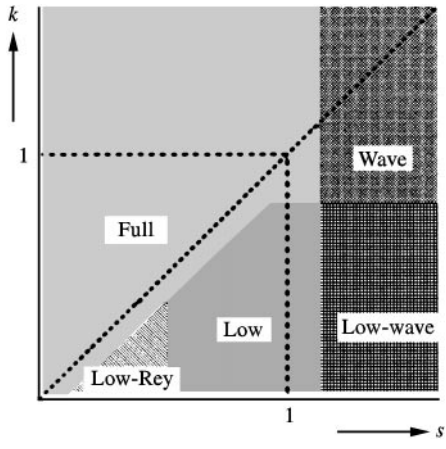

Figure 3. Parameter overview of models.

quantify. These models incorporate some additional effects compared to the low reduced frequency models. However, a parameter analysis shows that if a more sophisticated model is desired, in fact all the terms have to be accounted for. The complete parameter range is covered by the low reduced frequency model and the full linearized Navier–Stokes model. One can summarize the ranges of validity for the linear viscothermal models and the general wave equation as follows: $s \gg 1$, wave equation (wave); $k \ll 1$ and $k/s \ll 1$, low reduced frequency (Low); $k \ll 1$ and $k/s \ll 1$ and $s \ll 1$, low reduced frequency, Reynolds equation (Low-Rey); $k \ll 1$ and $k/s \ll 1$ and $s \gg 1$, low reduced frequency, modified wave equation (Low-wave); arbitrary k and s, full linearized Navier–Stokes (Full).[†]

A graphical representation of these ranges of validity is given in Figure 3. It is stressed that in each area the most efficient model is given. One could for instance use the full model for all situations, but clearly for $k \ll 1$ and $k/s \ll 1$ the low reduced frequency model is far more efficient.

For the case of arbitrary k but $k/s \ll 1$ the simplified wave numbers, as described in section 3.3 could be used. However, assuming $k/s \ll 1$ immediately suggests that another model, i.e., the low reduced, modified wave or wave, would be more efficient (see Figure 3). This assumption, which is often used by authors who use a full linearized Navier–Stokes model, at the same time eliminates the actual need for the full model. Only for the most general case of arbitrary k and k/s should the full model be used. Note that for $s \gg 1$ the general wave equation can be used.

6.2. PRACTICAL IMPLICATIONS

The key quantities of interest for a good choice of the appropriate model are obviously k and k/s. In physical terms these quantities represent the ratio between

[†]The full linearized Navier–Stokes with simpified wave numbers is valid for $k/s \ll 1$. It can easily be seen in the graph that this is not an efficient model. Hence, it is not included.

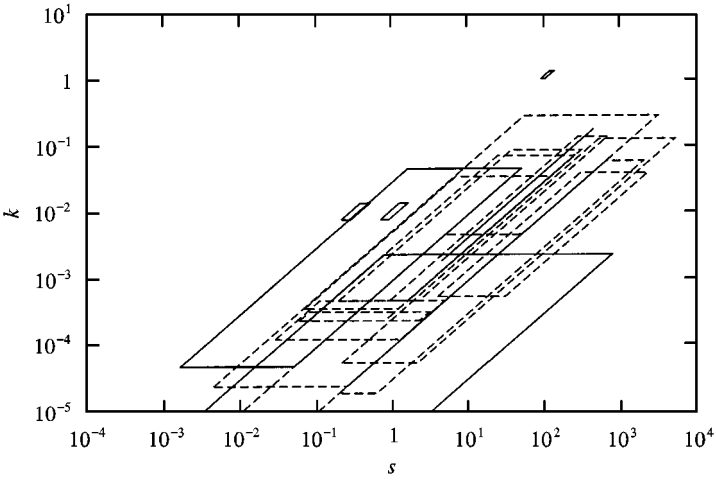

Figure 4. Dimensionless parameters in the literature: calculations (—), experiments (– –).

the length scale l and the acoustic wavelength, and the ratio between the boundary layer thickness and the acoustic wavelength respectively. An interesting point is the analysis of these terms. For $s \leqslant 1$ and $k/s \geqslant 1$ for instance the full model should be used. The question now arises whether or not these conditions are of any practical interest. With the dimensionless parameters one can write

$$s = l\sqrt{\rho_0 \omega/\mu}\,, \quad k/s = \sqrt{\mu\omega/\rho_0 c_0^2}\,. \tag{33}$$

For gases under atmospheric conditions, the speed of sound is of the order of magnitude of 5×10^2 m/s, the density is of the order of 1 kg/m^3 and the viscosity is of the order of 10^{-5} Ns/m^2. By varying the frequency or the length scale, the shear wave number can vary from low to very high values. Expression (33) shows that the frequency is the only variable quantity in k/s: it does not depend on the length scale l. For gases under atmospheric conditions, k/s exceeds unity only for frequencies higher than 10^9 Hz. However, for these high frequencies the medium can no longer be regarded as homogeneous and one of the basic assumptions described in section 2.1, is violated.

This can be illustrated with the following simple example. By using expression (33), the basic conditions $l > 10^{-7}$ m and $f < 10^9$ Hz can be expressed in terms of k/s and s as

$$f < 10^9 \text{ Hz}, \quad \left(\frac{k}{s}\right) < \sqrt{\frac{2\pi\mu}{\rho_0 c_0^2} \times 10^9}; \quad l > 10^{-7} \text{ m}, \quad s > \frac{\rho_0 c_0}{\mu} \times 10^{-7} \left(\frac{k}{s}\right). \tag{34}$$

For air under atmospheric conditions this gives

$$(k/s) < 0{\cdot}3\pi, \qquad s > 2{\cdot}24\,(k/s). \tag{35}$$

Thus, the full linearized Navier–Stokes model is not even valid in the major range where it should be of use for air under atmospheric conditions.

For fluids this reasoning also holds. The quantity k/s contains the ratio between the viscosity and the density. For fluids the viscosity is higher, but compared to gases the ratio between viscosity and density is of the same order of magnitude. Furthermore, the speed of sound in fluids is generally higher. This implies that for fluids the condition $k/s \ll 1$ will also usually be satisfied. If this condition is not satisfied one has to ensure that the basic assumptions are not violated.

This simple analysis shows that the practical importance of the full model is very limited. Only under extreme conditions, e.g. at low temperatures or low pressures, one encounters situations were the full model should be used.† However, one has to ensure that the basic assumptions are not violated in these cases. This leads to the perhaps surprising conclusion that for gases under atmospheric conditions the full linearized Navier–Stokes model is not valid in the parameter range where it should be of use. Most viscothermal problems can be handled with the low reduced frequency models. In fact, a number of papers indicate the necessity of a full model because of the high frequencies involved, whereas a low reduced frequency model would have been sufficient [42, 44, 45]. Some examples will be presented in Part II of the present paper.

6.3. OVERVIEW OF THE LITERATURE FOR LAYERS

The dimensionless parameters are used to analyse the literature for the layer geometry. The overview is based on the references presented in Tables 1–3. For this purpose, the values of the dimensionless parameters at which the calculations and experiments were performed were determined from the data given in the references [42, 44, 45, 48, 50, 67, 68, 58–60, 52, 65].

The graph clearly shows that for all investigations the low reduced frequency models, modified wave equation models or general wave equation models would have been sufficient. None of the present cases required a more sophisticated model, such as the full linearized Navier–Stokes model. The conclusion to be drawn from this figure is that, although a variety of models has been developed, this was not necessary when taking a critical look at the dimensionless parameters. Some investigations mentioned in Tables 1 and 2 could have been carried out with much simpler models. Analysis of the values of the parameters, listed in tables, also immediately reveals that the conditions for the use of simpler models are satisfied.

7. CONCLUSIONS

The conclusions to be drawn from the present investigation are as follows.

Viscothermal wave propagation is governed by a number of dimensionless parameters. The most important parameters are the shear wave number, s, and the reduced frequency, k

†For these cases situations are encountered where the jump conditions must be applied at the boundaries, see section 2.2.

The viscothermal models presented in the literature, can be grouped into three categories: full linearized Navier–Stokes models, simplified Navier–Stokes models and low reduced frequency models. The range of validity of the models is governed by the values of k and k/s

The full linearized Navier–Stokes model should only be used under extreme conditions. For gases under atmospheric conditions, this model is not even valid in the range of use because the basic assumptions are violated

The assumption of small k/s, as often used in the literature concerning full models, actually eliminates the need for a full model

The simplified Navier–Stokes models are redundant: the complete parameter range is covered by the other models

The low reduced frequency model can be used for most problems. Because of the simplicity of this model, models are already available that include the full acousto-elastic coupling for complex geometries. The model is valid for $k \ll 1$ and $k/s \ll 1$.

In the literature a variety of models was presented for the squeeze film damping problem. Several authors stated that for miniaturized transducers, the full model had to be used because of the high frequencies involved. An analysis of the parameters shows that for all literature concerning squeeze film problems, treated in this paper, a simple low reduced frequency model is sufficient and the most efficient.

ACKNOWLEDGMENTS

The author would like to thank Henk Tijdeman, Ruud Spiering, Peter van der Hoogt, Bert Wolbert, Tom Basten, Frits van der Eerden, Diemer de Vries, Leen van Wijngaarden, Jan Verheij, Piet Zandbergen, Jean Pierre Coyette and Bart Paarhuis for their valuable suggestions and comments.

REFERENCES

1. J. W. S. Rayleigh 1945 *The Theory of Sound*, Vol. II, New York: Dover, second revised edition.
2. W. S. Griffin, H. H. Richardson and S. Yamanami 1966 *Journal of Basic Engineering* 451–456. A study of fluid squeeze-film damping.
3. S. M. R. Hashemi and B. J. Roylance 1989 *Tribology Transactions* **32**, 461–468. Analysis of an oscillatory oil squeeze film including effects of fluid inertia.
4. E. C. Kuhn and C. C. Yates 1964 *ASLE Transactions* **7**, 299–303. Fluid inertia effect on the film pressure between axially oscillating parallel circular plates.
5. J. Prakash and H. Christensen 1978 *Journal of Mechanical Engineering Science* **20**, 183–188. Squeeze film between two rough rectangular plates.
6. P. Sinha and C. Singh 1982 *Applied Scientific Research* **39**, 169–179. Micropolar squeeze film between rough rectangular plates.
7. R. M. Terrill 1969 *Journal of Lubrication Technology* **91**, 126–131. The flow between two parallel circular discs, one of which is subject to a normal sinusoidal oscillation.
8. J. A. Tichy and M. F. Modest 1978 *Journal of Lubrication Technology*, **100**, 316–322. Squeeze film flow between arbitrary two-dimensional surfaces subject to normal oscillations.

9. J. A. Tichy 1984 *ASLE Transactions* **28**, 520–526. Measurements of squeeze-film bearing forces and pressures, including the effect of fluid inertia.
10. J. V. Beck, W. G. Holliday and C. L. Strodtman 1969 *Journal of Lubrication Technology* **91**, 138–148. Experiments and analysis of a flat disk squeeze-film bearing including effects of supported mass motion.
11. V. Ramamurthy and U. S. Rao 1987 *Fluid Dynamics Research*, **2**, 47–63. The steady streaming generated by a vibrating plate parallel to a fixed plate in a dusty fluid.
12. C. Y. Wang and B. Drachman 1982 *Applied Scientific Research* **39**, 55–68. The steady streaming generated by a vibrating plate parallel to a fixed plate.
13. N. Rott 1974 *Journal of Applied Mathematics and Physics* **25**, 417. The influence of heat conduction on acoustic streaming.
14. P. Merkli and H. Thomann 1975 *Journal of Fluid Mechanics* **68**, 567–575. Transition to turbulence in oscillating pipe flow.
15. G. Maidanik 1966 *Journal of the Acoustical Society of America* **40**, 1064–1072. Energy dissipation associated with gas-pumping in structural joints.
16. E. E. Ungar and J. R. Carbonell 1966 *AIAA Journal* **4**, 1385–1390. On panel vibration damping due to structural joints.
17. S. Makarov and M. Ochmann 1996 *Acustica* **82**, 579–606. Non-linear and thermoviscous phenomena in acoustics, Part I.
18. S. Makarov and M. Ochmann 1997 *Acustica* **83**, 197–222. Non-linear and thermoviscous phenomena in acoustics, Part II.
19. S. Makarov and M. Ochmann 1997 *Acustica* **83**, 827–846. Non-linear and thermoviscous phenomena in acoustics, Part III.
20. G. P. J. Too and S. T. Lee 1995 *Journal of the Acoustical Society of America* **97**, 867–874. Thermoviscous effects on transient and steady-state sound beams using non-linear progressive wave equation models.
21. H. Tijdeman 1975 *Journal of Sound and Vibration* **39**, 1–33 . On the propagation of sound waves in cylindrical tubes.
22. K. Rathnam and M. M. Oberai 1978 *Journal of Sound and Vibration* **60**, 379–388. Acoustic wave propagation in cylindrical tubes containing slightly rarefied gases.
23. K. Rathnam 1985 *Journal of Sound and Vibration* **103**, 448–452. Influence of velocity slip and temperature jump in rarefied gas acoustic oscillations in cylindrical tubes.
24. M. Moldover, J. Mehl and M. Greenspan 1986 *Journal of the Acoustical Society of America* **79**, 253–270. Gas-filled spherical resonators: theory and experiment.
25. M. J. Anderson and P. G. Vaidya 1989 *Journal of the Acoustical Society of America* **86**, 2385–2396. Sound propagation in a waveguide with finite thermal conduction at the boundary.
26. H. S. Roh, W. P. Arnot and J. M. Sabatier 1991 *Journal of the Acoustical Society of America* **89**, 2617–2624. Measurements and calculation of acoustic propagation constants in arrays of small air-filled rectangular tubes.
27. N. Rott 1969 *Journal of Applied Mathematics and Physics* **20**, 230. Damped and thermally driven acoustic oscillations.
28. N. Rott 1973 *Journal of Applied Mathematics and Physics* **24**, 24. Thermally driven acoustic oscillations, Part II: stability limit for helium.
29. N. Rott 1975 *Journal of Applied Mathematics and Physics* **26**, 43. Thermally driven acoustic oscillations, Part III: second-order heat flux.
30. N. Rott and G. Zouzoulas 1976 *Journal of Applied Mathematics and Physics* **27**, 197. Thermally driven acoustic oscillations, Part IV: tubes with variable cross-section.
31. G. Zouzoulas and N. Rott 1976 *Journal of Applied Mathematics and Physics* **27**, 325. Thermally driven acoustic oscillations, Part V: gas–liquid oscillations.
32. R. Raspet, H. E. Bass and J. Kordomenos 1993 *Journal of the Acoustical Society of America* **94**, 2232–2239. Thermoacoustics of travelling waves: theoretical analysis for a inviscid ideal gas.

33. J. Kordomenos, A. A. Atchley, R. Raspet and H. E. Bass 1995 *Journal of the Acoustical Society of America* **98**, 1623–1628. Experimental study of a thermoacoustic termination of a travelling-wave tube.
34. E. Stuhlträger and H. Thomann 1986 *Journal of Applied Mathematics and Physics* **37**, 155. Oscillations of a gas in an open-ended tube near resonance.
35. J. H. M. Disselhorst 1978 Ph.D. Thesis, *University of Twente, The Netherlands.* Acoustic resonance in open tubes.
36. M. P. Verge 1995 Ph.D. Thesis, *Technical University of Eindhoven, The Netherlands*, Aeroacoustics of confined jets.
37. U. Ingard 1967 *Journal of the Acoustical Society of America* **42**, Acoustic non-linearity of an orifice.
38. J. H. M. Disselhorst and L. van Wijngaarden 1980 *Journal of Fluid Mechanics* **99**, 293–319. Flow in the exit of open pipes during acoustic resonance.
39. C. A. M. Peters, A. Hirschberg, A. J. Reijen and A. P. J. Wijnands 1993 *Journal of Fluid Mechanics* **256**, 499–534. Damping and reflection coefficient measurements for an open pipe at low Mach and low Helmholtz numbers.
40. M. Bruneau, Ph. Herzog, J. Kergomard and J. D. Polack 1989 *Wave Motion* **11**, 441–451. General formulation of the dispersion equation in bounded visco-thermal fluid.
41. J. B. Mehl 1985 *Journal of the Acoustical Society of America* **78**, 782–788. Spherical acoustic resonator: effects of shell motion.
42. G. Plantier and M. Bruneau 1990 *Journal d'Acoustique* **3**, 243–250. Heat conduction effects on the acoustic response of a membrane separated by a very thin air film from a backing electrode.
43. M. Bruneau, A. M. Bruneau, and P. Hamery 1993 *Acustica* **1**, 227–234. An improved approach to modelling the behaviour of thin fluid films trapped between a vibrating membrane and a backing wall surrounded by a reservoir at the periphery.
44. P. Hamery, M. Bruneau and A. M. Bruneau 1994 *Journal de Physique IV* **4**, C5–213–C5–216. Mouvement d'une couche de fluide dissipatif en espace clos sous l'action d'une source étendue (in French).
45. C. Karra, M. B. Tahar, G. Marquette and M. T. Chau 1996 *Inter Noise* 96 (F. Allison Hill, R. Lawrence, editors) 3003–3006, Liverpool, United Kingdom. Boundary element analysis of problems of acoustic propagation in viscothermal fluid.
46. C. Karra and M. Ben Tahar 1997 *Journal of the Acoustical Society of America* **102**, 1311–1318. An integral equation formulation for boundary element analysis of propagation in viscothermal fluids.
47. C. Karra 1996 Private communication.
48. A. Trochidis 1982 *Acoustica* **51**, 201–212. Vibration damping due to air or liquid layers.
49. A. Trochidis 1977 Ph.D. Thesis, *ITA, Berlin.* Körperschalldämpfung durch Viscositätsverluste in Gasschichten bei Doppelplatten (in German).
50. M. Möser 1980 *Acustica* **46**, 210–217. Damping of structure born sound by the viscosity of a layer between to plates.
51. W. M. Beltman, P. J. M. van der Hoogt, R. M. E. J. Spiering and H. Tijdeman 1996 *ISMA* 21 *Conference on Noise and Vibration Engineering* (P. Sas, editor), 1605–1618, *Leuven, Belgium.* Energy dissipation in thin air layers.
52. W. M. Beltman, P. J. M. van der Hoogt, R. M. E. J. Spiering and H. Tijdeman 1998 *Journal of Sound and Vibration* **216**, 159–185. Implementation and experimental validation of a new viscothermal acoustic finite element for acousto-elastic problems.
53. R. M. S. M. Schulkes 1990 *Technical Report* 90-46, *Delft University of Technology, Faculty of Technical Mathematics and Informatics, Delft, The Netherlands.* Interactions of an elastic solid with a viscous fluid: eigenmode analysis.
54. R. M. S. M. Schulkes 1989 *Technical Report* 89-69, *Delft University of Technology, Faculty of Technical Mathematics and Informatics, Delft, The Netherlands.* Fluid oscillations in an open, flexible container.

55. M. R. Stinson 1991 *Journal of the Acoustical Society of America* **89**, 550–558. The propagation of plane sound waves in narrow and wide circular tubes, and generalization to uniform tubes of arbitrary cross-section.
56. A. Cummings 1993 *Journal of Sound and Vibration* **162**, 27–42. Sound propagation in narrow tubes of arbitrary cross-section.
57. A. D. Lapin 1996 *Acoustical Physics*, **42**, 509–511. Integral relations for acoustic modes in a channel with arbitrary cross-section.
58. M. J. H. Fox and P. N. Whitton 1980 *Journal of Sound and Vibration* **73**, 279–295. The damping of structural vibrations by thin gas films.
59. T. Önsay 1993 *Journal of Sound and Vibration* **163**, 231–259. Effects of layer thickness on the vibration response of a plate-fluid layer system.
60. T. Önsay 1994 *Journal of Sound and Vibration* **178**, 289–313. Dynamic interaction between the bending vibrations of a plate and a fluid layer attenuator.
61. P. Lotton, L. Husník, A. M. Bruneau and Z. Škvor 1994 *Journal de Physique IV* **4**, C5–217–C5–220. Modèle à constantes localisées de transducteurs: dissipation dans les couches limites (in French).
62. M. Bruneau, A. M. Bruneau, Z. Škvor and P. Lotton 1994. *Acustica* **2**, 223–232. An equivalent network modelling the strong coupling between a vibrating membrane and a fluid film.
63. M. Bruneau, A. M. Bruneau and P. Dupire 1995 *Acta acustica* **3**, 275–282. A model for rectangular miniaturized microphones.
64. W. M. Beltman, P. J. M. van der Hoogt, R. M. E J. Spiering and H. Tijdeman 1997 *Journal of Sound and Vibration* **206**, 217–241. Air loads on a rigid plate oscillating normal to a fixed surface.
65. W. M. Beltman, P. J. M. van der Hoogt, R. M. E J. Spiering and H. Tijdeman 1996 in *Conference on Spacecraft Structures, Materials and Mechanical Testing* (W. R. Burke, editor) 219–226, *Noordwijk, The Netherlands.* Air loads on solar panels during launch. ESA SP-386.
66. W. M. Beltman 1996 *Journal of the Dutch Acoustical Society* (*NAG*) **131**, 27–38. Damping of double wall panels (in Dutch).
67. L. C. Chow and R. J. Pinnington 1987 *Journal of Sound and Vibration* **118**, 123–139. Practical industrial method of increasing structural damping in machinery, I: squeeze film damping with air.
68. L. C. Chow and R. J. Pinnington 1989 *Journal of Sound and Vibration* **128**, 333–347. Practical industrial method of increasing structural damping in machinery, II: squeeze film damping with liquids.
69. M. Bruneau, J. D. Polack, Ph. Herzog and J. Kergomard 1990 *Colloque de Physique* **51**, C2-17–C2–20. Formulation générale des équations de propagation et de dispersion des ondes sonores dans les fluides viscothermique (in French).
70. M. Bruneau 1994 *Journal de Physique IV* **4**, C5–675–C5–684. Acoustique des cavités: modèles et applications (in French).
71. A. M. Bruneau, M. Bruneau, Ph. Herzog and J. Kergomard 1987 *Journal of Sound and Vibration* **119**, 15–27. Boundary layer attenuation of higher order modes in waveguides.
72. H. A. Scarton and W. T. Rouleau 1973 *Journal of Fluid Mechanics* **58**, 595–621. Axisymmetric waves in compressible Newtonian liquids contained in rigid tubes: steady-periodic mode shapes and dispersion by the method of eigenvalleys.
73. P. N. Liang and H. A. Scarton 1994 *Journal of Sound and Vibration* **177**, 121–135. Three-dimensional mode shapes for higher order circumferential thermoelastic waves in an annular elastic cylinder.

APPENDIX A: GEOMETERIES, CO-ORDINATE SYSTEMS AND FUNCTIONS

A.1. SPHERE

The basic geometrical dimensions and operators are (see Figure A.1)

$$l = R, \quad \mathbf{x} = (r, \theta, \phi), \qquad r = \bar{r}/R\,, \qquad \theta = \bar{\theta}, \qquad \phi = \bar{\phi},$$

$$\nabla = \mathbf{e}_r \frac{\partial}{\partial r} + \mathbf{e}_\theta \frac{1}{r}\frac{\partial}{\partial \theta} + \mathbf{e}_\phi \frac{1}{r\sin(\theta)}\frac{\partial}{\partial \phi}\,,$$

$$\Delta = \frac{1}{r^2}\frac{\partial}{\partial r}\left[r^2 \frac{\partial}{\partial r}\right] + \frac{1}{r^2 \sin(\theta)}\frac{\partial}{\partial \theta}\left[\sin(\theta)\frac{\partial}{\partial \theta}\right] + \frac{1}{r^2 \sin(\theta)}\frac{\partial^2}{\partial \phi^2}\,. \tag{A.1}$$

A.2. CIRCULAR TUBE

The basic geometrical dimensions and operators are (see Figure A.2)

$$l = R, \qquad \mathbf{x} = (r, \theta, x), \qquad r = \bar{r}/R\,, \qquad \theta = \bar{\theta}, \qquad x = \omega \bar{x}/c_0\,,$$

$$\nabla = \mathbf{e}_r \frac{\partial}{\partial r} + \mathbf{e}_\theta \frac{1}{r}\frac{\partial}{\partial \theta} + \mathbf{e}_x k \frac{\partial}{\partial x}\,, \qquad \Delta = \frac{\partial^2}{\partial r^2} + \frac{1}{r}\frac{\partial}{\partial r} + \frac{1}{r^2}\frac{\partial^2}{\partial \theta^2} + k^2 \frac{\partial^2}{\partial x^2}\,, \tag{A.2}$$

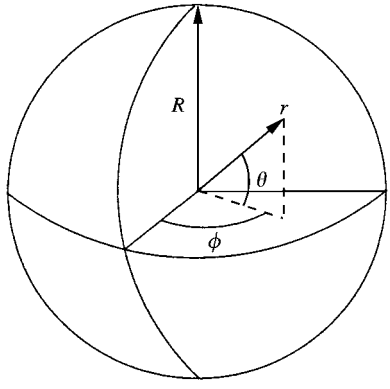

Figure A.1. Geometry of sphere.

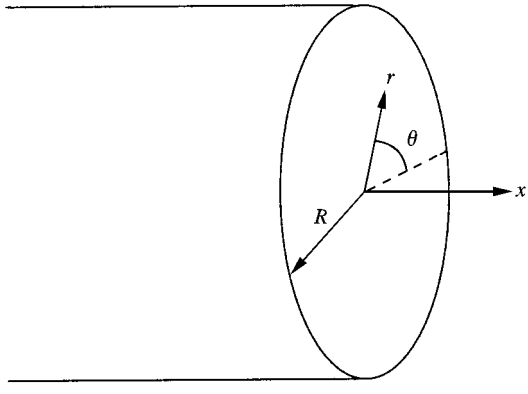

Figure A.2. Geometry of circular tube.

TABLE A.1

Expressions for circular tube

	Total	Low s	High s
A	$\dfrac{J_0(sri\sqrt{i})}{J_0(si\sqrt{i})} - 1$	$-\dfrac{1}{4} is^2 [1 - r^2]$	-1
B	$\dfrac{J_2(si\sqrt{i})}{J_0(si\sqrt{i})}$	$-\dfrac{1}{8} is^2$	-1
$\Re$	$\dfrac{1}{\pi}\int_{\theta=0}^{2\pi} v_r(x, 1, \theta)\,d\theta$		

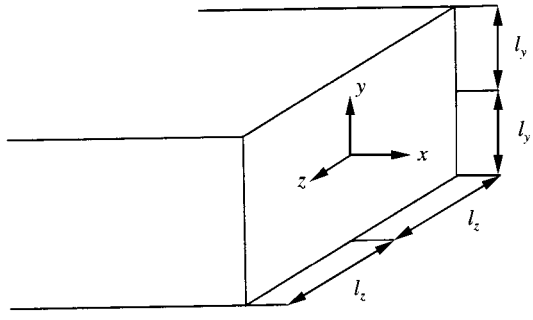

Figure A.3. Geometry of rectangualr tube.

The operators for the low reduced frequency model are

$$\mathbf{x}^{cd} = (r, \theta), \qquad \mathbf{x}^{pd} = (x), \qquad \nabla^{cd} = \mathbf{e}_r \frac{\partial}{\partial r} + \mathbf{e}_\theta \frac{1}{r}\frac{\partial}{\partial \theta},$$

$$\nabla^{pd} = \mathbf{e}_x k \frac{\partial}{\partial x}, \qquad \Delta^{cd} = \frac{\partial^2}{\partial r^2} + \frac{1}{r}\frac{\partial}{\partial r} + \frac{1}{r^2}\frac{\partial^2}{\partial \theta^2}, \qquad \Delta^{pd} = k^2 \frac{\partial^2}{\partial x^2}. \tag{A.3}$$

The functions that are used in the low reduced frequency model are given in Table A.1.

A.3. RECTANGULAR TUBE

The basic geometrical dimensions and operators are (see Figure A.3).

$$l = l_y, \quad \mathbf{x} = (x, y, z), \quad a = l_z/l_y, \quad x = \omega\bar{x}/c_0, \quad y = \bar{y}/l_y, \quad z = \bar{z}/l_y,$$

$$\nabla = \mathbf{e}_x k \frac{\partial}{\partial x} + \mathbf{e}_y \frac{\partial}{\partial y} + \mathbf{e}_z \frac{\partial}{\partial z}, \qquad \Delta = k^2 \frac{\partial^2}{\partial x^2} + \frac{\partial^2}{\partial y^2} + \frac{\partial^2}{\partial z^2}. \tag{A.4}$$

TABLE A.2

Expressions for rectangular tube

	Total	Low s	High s
A	$Q_1 \sum_{q=1,3\ldots}^{\infty} \frac{(-1)^{\frac{q-1}{2}}}{qQ_2^2}\left[\frac{\cosh(Q_2 z)}{\cosh(Q_2)} - 1\right]\cos\left(\frac{q\pi y}{2}\right)$	$Q_1 \sum_{q=1,3\ldots}^{\infty} \frac{(-1)^{\frac{q-1}{2}}}{q\hat{Q}_2^2}\left[\frac{\cosh(\hat{Q}_2 z)}{\cosh(\hat{Q}_2)} - 1\right]\cos\left(\frac{q\pi y}{2}\right)$	-1
	$Q_1 = \frac{\mathrm{i}a^2 s^2 4}{\pi}; \quad Q_2 = a\sqrt{\left(\frac{q\pi}{2}\right)^2 + \mathrm{i}s^2}$	$Q_1 = \frac{\mathrm{i}a^2 s^2 4}{\pi}; \quad \hat{Q}_2 = a\frac{q\pi}{2}$	
B	$Q_1 \sum_{q=1,3\ldots}^{\infty} \frac{(-1)^{\frac{q-1}{2}}}{q^2 Q_2^2}\left[\frac{\tanh(aQ_2)}{aQ_2} - 1\right]$	$Q_1 \sum_{q=1,3\ldots}^{\infty} \frac{(-1)^{\frac{q-1}{2}}}{q^2 \hat{Q}_2^2}\left[\frac{\tanh(a\hat{Q}_2)}{a\hat{Q}_2} - 1\right]$	-1
	$Q_1 = \frac{\mathrm{i}a^2 s^2 8}{\pi^2}; \quad Q_2 = a\sqrt{\left(\frac{q\pi}{2}\right)^2 + \mathrm{i}s^2}$	$Q_1 = \frac{\mathrm{i}a^2 s^2 8}{\pi^{12}}; \quad \hat{Q}_2 = a\frac{q\pi}{2}$	
$\mathfrak{R}$	$\frac{1}{4}\int_{z=-1}^{1} [v_y(x, 1, z) - v_y(x, -1, z)]\,\mathrm{d}z$		
	$+ \frac{1}{4}\frac{1}{a}\int_{y=-1}^{1} [v_z(x, y, 1) - v_z(x, y, -1)]\,\mathrm{d}y$		

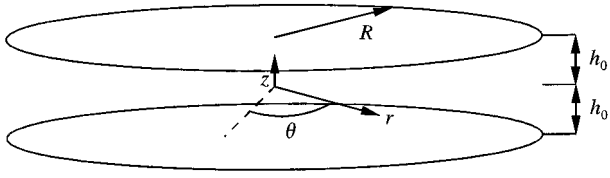

Figure A.4. Geometry of the circular layer.

TABLE A.3

Expressions for the circular layer

	Total	Low s	High s
A	$\dfrac{\cosh(sz\sqrt{\mathrm{i}})}{\cosh(s\sqrt{\mathrm{i}})} - 1$	$\dfrac{1}{2}\mathrm{i}s^2\left[\dfrac{1}{3}z^2 - 1\right]$	-1
B	$\dfrac{\tanh(s\sqrt{\mathrm{i}})}{s\sqrt{\mathrm{i}}} - 1$	$-\dfrac{1}{3}\mathrm{i}s^2$	-1
$\mathfrak{R}$	$\dfrac{1}{2}[v_z(x, y, 1) - v_z(x, y, -1)]$		

The operators for the low reduced frequency model are

$$\mathbf{x}^{cd} = (y, z), \qquad \mathbf{x}^{pd} = (x), \qquad \boldsymbol{\nabla}^{cd} = \mathbf{e}_x k \frac{\partial}{\partial x}, \qquad \boldsymbol{\nabla}^{pd} = \mathbf{e}_y \frac{\partial}{\partial y} + \mathbf{e}_z \frac{\partial}{\partial z},$$

$$\Delta^{cd} = \frac{\partial^2}{\partial y^2} + \frac{\partial^2}{\partial z^2}, \qquad \Delta^{pd} = k^2 \frac{\partial^2}{\partial x^2}. \tag{A.5}$$

The functions that are used in the low reduced frequency model are given in Table A.2.

A.4. CIRCULAR LAYER

The basic geometrical dimensions and operators are (see Figure A.4).

$$l = h_0, \quad \mathbf{x} = (r, \theta, z), \quad r = \omega\bar{r}/c_0, \quad \theta = \bar{\theta}, \qquad z = \bar{z}/h_0,$$

$$\boldsymbol{\nabla} = \mathbf{e}_r k \frac{\partial}{\partial r} + \mathbf{e}_\theta k \frac{1}{r}\frac{\partial}{\partial \theta} + \mathbf{e}_z \frac{\partial}{\partial z}, \qquad \Delta = k^2 \frac{\partial^2}{\partial r^2} + k^2 \frac{1}{r}\frac{\partial}{\partial r} + k^2 \frac{1}{r^2}\frac{\partial^2}{\partial \theta^2} + \frac{\partial^2}{\partial z^2}. \tag{A.6}$$

The operators for the low reduced frequency model are

$$\mathbf{x}^{cd} = (z), \qquad \mathbf{x}^{pd} = (r, \theta), \qquad \boldsymbol{\nabla}^{cd} = \mathbf{e}_z \frac{\partial}{\partial z}, \qquad \boldsymbol{\nabla}^{pd} = \mathbf{e}_r k \frac{\partial}{\partial r} + \mathbf{e}_\theta k \frac{1}{r}\frac{\partial}{\partial \theta},$$

$$\Delta^{cd} = \frac{\partial^2}{\partial z^2}, \qquad \Delta^{pd} = k^2 \frac{\partial^2}{\partial r^2} + k^2 \frac{1}{r}\frac{\partial}{\partial r} + k^2 \frac{1}{r^2}\frac{\partial^2}{\partial \theta^2}. \tag{A.7}$$

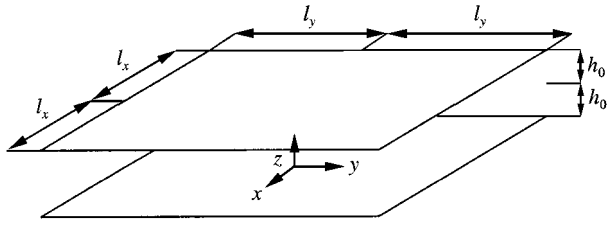

Figure A.5. Geometry of the rectangular layer.

TABLE A.4

Expressions for the rectangular layer

	Total	Low s	High s
A	$\dfrac{\cosh(sz\sqrt{\mathrm{i}})}{\cosh(s\sqrt{\mathrm{i}})} - 1$	$\dfrac{1}{2}\mathrm{i}s^2\left[\dfrac{1}{3}z^2 - 1\right]$	-1
B	$\dfrac{\tanh(s\sqrt{\mathrm{i}})}{s\sqrt{\mathrm{i}}} - 1$	$-\dfrac{1}{3}\mathrm{i}s^2$	-1
$\mathfrak{R}$	$\dfrac{1}{2}[v_z(x, y, 1) - v_z(x, y, -1)]$		

The functions that are used in the low reduced frequency model are given in Table A.3.

A.5. RECTANGULAR LAYER

The basic geometrical dimensions and operators are (see Figure A.5).

$$l = h_0, \quad \mathbf{x} = (x, y, z), \quad a = l_y/l_x, \quad x = \omega\bar{x}/c_0\,, \quad y = \omega\bar{y}/c_0\,, \quad z = \bar{z}/h_0\,,$$

$$\boldsymbol{\nabla} = \mathbf{e}_x k\frac{\partial}{\partial x} + \mathbf{e}_y k\frac{\partial}{\partial y} + \mathbf{e}_z\frac{\partial}{\partial z}\,, \tag{A.8}$$

$$\Delta = k^2\frac{\partial^2}{\partial x^2} + k^2\frac{\partial^2}{\partial y^2} + \frac{\partial^2}{\partial z^2}\,. \tag{A.9}$$

The operators for the low reduced frequency model are

$$\mathbf{x}^{cd} = (z), \quad \mathbf{x}^{pd} = (x, y), \quad \boldsymbol{\nabla}^{cd} = \mathbf{e}_z\frac{\partial}{\partial z}\,, \quad \boldsymbol{\nabla}^{pd} = \mathbf{e}_x k\frac{\partial}{\partial x} + \mathbf{e}_y k\frac{\partial}{\partial y}\,,$$

$$\Delta^{cd} = \frac{\partial^2}{\partial z^2}\,, \qquad \Delta^{pd} = k^2\frac{\partial^2}{\partial x^2} + k^2\frac{\partial^2}{\partial y^2}\,. \tag{A.10}$$

The functions that are used in the low reduced frequency model are given in Table A.4.

APPENDIX B: NOMENCLATURE

A	function describing velocity and temperature profiles
A_{aq}, B_{aq}, A_{hq}, B_{hq}	constants
A^{cd}	dimensionless cross-sectional area
∂A^{cd}	dimensionless area of cross-section boundary
$B(s)$	function accounting for viscous or thermal effects
$a = l_y/l_x$	aspect ratio
C	function describing the temperature profile
C_p	specific heat at constant pressure
C_v	specific heat at constant volume
c_0	undisturbed speed of sound
D	function describing the temperature profile
$\mathbf{e}_n$	unit normal vector
$\mathbf{e}_r$	unit vector in the r direction
$\mathbf{e}_x$	unit vector in the x direction
$\mathbf{e}_y$	unit vector in the y direction
$\mathbf{e}_z$	unit vector in the z direction
$\mathbf{e}_\theta$	unit vector in the θ direction
$\mathbf{e}_\phi$	unit vector in the ϕ direction
h_0	half-layer thickness
$\mathrm{i} = \sqrt{-1}$	imaginary unit
j_n	spherical Bessel function of order n
$\mathbf{J}_m$	Bessel function of the first kind, order m
$k = \omega l/c_0$	reduced frequency
k_a	acoustic wave number
k_h	entropic wave number
k_v	rotational wave number
l	characteristic length scale
l_x	half-length in the x direction
l_y	half-length in the y direction
l_z	half-length in the z direction
$n(s\sigma)$	polytropic constant
$\bar{p} = p_0\,[1 + p\mathrm{e}^{\mathrm{i}\omega t}]$	pressure
p_0	mean pressure
p	dimensionless pressure amplitude
R	radius
$\Re$	squeeze term
R_0	gas constant
$\bar{r}$	radial co-ordinate
r	dimensionless radial co-ordinate
$s = l\sqrt{\rho_0\omega/\mu}$	shear wave number
$\bar{T} = T_0\,[1 + T\mathrm{e}^{\mathrm{i}\omega t}]$	temperature
T_0	mean temperature
T	dimensionless temperature amplitude
T_a	acoustic temperature
T_h	entropic temperature
t	time
$\bar{\mathbf{v}} = c_0\mathbf{v}\mathrm{e}^{\mathrm{i}\omega t}$	velocity vector
$\mathbf{v}$	dimensionless amplitude of the velocity vector
v	dimensionless amplitude of the velocity
$\mathbf{v}_l$	solenoidal velocity vector
$\mathbf{v}_{la}$	acoustic part of selenoidal velocity vector
$\mathbf{v}_{lh}$	entropic part of selenoidal velocity vector

$\mathbf{v}_v$	rotational velocity vector
v_r	dimensionless velocity component in the r direction
v_x	dimensionless velocity component in the x direction
v_y	dimensionless velocity component in the y direction
v_z	dimensionless velocity component in the z direction
v_θ	dimensionless velocity component in the θ direction
v_ϕ	dimensionless velocity component in the ϕ direction
$\mathbf{v}^{cd}$	velocity vector in the *cd* directions
$\mathbf{v}^{pd}$	velocity vector in the *pd* directions
$\mathbf{x}$	spatial co-ordinates
$\mathbf{x}^{cd}$	cross-sectional co-ordinates
$\mathbf{x}^{pd}$	propagation co-ordinates
Γ	propagation constant
$\gamma = C_p/C_v$	ratio of specific heats
η	bulk viscosity
$\bar{\theta}$	co-ordinate in the θ direction
θ	dimensionless co-ordinate in the θ direction
Λ_a	constant
Λ_h	constant
λ	thermal conductivity
μ	dynamic viscosity
ξ	viscosity ratio
$\bar{\rho} = \rho_0 [1 + \rho e^{i\omega t}]$	density
ρ_0	mean density of air
ρ	dimensionless density amplitude
$\sigma = \sqrt{\mu C_p/\lambda}$	square root of the Prandtl number
Φ	viscous dissipation function
$\bar{\phi}$	co-ordinate in the ϕ direction
ϕ	dimensionless co-ordinate in the ϕ direction
ω	angular frequency
$\bar{\nabla}$	gradient operator
∇	dimensionless gradient operator
∇^{cd}	dimensionless gradient operator in the *cd* directions
∇^{pd}	dimensionless gradient operator in the *pd* directions
$\bar{\Delta}$	Laplace operator
Δ	dimensionless Laplace operator
Δ^{cd}	dimensionless Laplace operator in the *cd* directions